First Millimeter Detection of the Disk around a Young, Isolated, Planetary-mass Object

Amelia Bayo[1], Viki Joergens[2], Yao Liu[2,3], Robert Brauer[4], Johan Olofsson[1,2], Javier Arancibia[1], Paola Pinilla[5], Sebastian Wolf[4], Jan Philipp Ruge[4], Thomas Henning[2], Antonella Natta[6,7], Katharine G. Johnston[8], Mickael Bonnefoy[9], Henrik Beuther[2], and Gael Chauvin[9,10]

[1] Instituto de Física y Astronomía, Facultad de Ciencias, Universidad de Valparaíso, Av. Gran Bretaña 1111, Valparaíso, Chile; ameia.bayo@uv.cl
[2] Max Planck Institut für Astronomie, Königstuhl 17, D-69117 Heidelberg, Germany
[3] Purple Mountain Observatory, and Key Laboratory for Radio Astronomy, Chinese Academy of Sciences, 2 West Beijing Road, Nanjing 210008, China
[4] Institute of Theoretical Physics and Astrophysics, University of Kiel, Leibnizstr. 15, D-24118 Kiel, Germany
[5] Department of Astronomy/Steward Observatory, The University of Arizona, 933 North Cherry Avenue, Tucson, AZ 85721, USA
[6] School of Cosmic Physics, Dublin Institute for Advanced Studies, 31 Fitzwilliams Place, Dublin 2, Ireland
[7] INAF-Osservatorio Astrofisico di Arcetri, L.go E. Fermi 5, I-50125 Firenze, Italy
[8] School of Physics and Astronomy, E.C. Stoner Building, The University of Leeds, Leeds LS2 9JT, UK
[9] Univ. Grenoble Alpes, CNRS, IPAG, F-38000 Grenoble, France
[10] Unidad Mixta Internacional Franco-Chilena de Astronomía, CNRS/INSU UMI 3386 and Departamento de Astronomía, Universidad de Chile, Casilla 36-D, Santiago, Chile

Abstract

OTS44 is one of only four free-floating planets known to have a disk. We have previously shown that it is the coolest and least massive known free-floating planet ($\sim 12\ M_{\rm Jup}$) with a substantial disk that is actively accreting. We have obtained Band 6 (233 GHz) ALMA continuum data of this very young disk-bearing object. The data show a clear unresolved detection of the source. We obtained disk-mass estimates via empirical correlations derived for young, higher-mass, central (substellar) objects. The range of values obtained are between 0.07 and 0.63 $M_\oplus$ (dust masses). We compare the properties of this unique disk with those recently reported around higher-mass (brown dwarfs) young objects in order to infer constraints on its mechanism of formation. While extreme assumptions on dust temperature yield disk-mass values that could slightly diverge from the general trends found for more massive brown dwarfs, a range of sensible values provide disk masses compatible with a unique scaling relation between $M_{\rm dust}$ and M_* through the substellar domain down to planetary masses.

Key words: brown dwarfs – stars: formation – stars: low-mass – stars: pre-main sequence

1. Introduction

Key questions are still unanswered about how low-mass stars come to emerge and gain their masses from their natal molecular clouds, but when we move toward the substellar domain (with masses below the hydrogen-burning mass limit, $\leqslant 0.072\ M_\odot$), these questions become even more fundamental.

Several scenarios have been proposed to prevent a substellar core in a dense environment from accreting to stellar mass (e.g., dynamical interactions, Reipurth & Clarke 2001; Umbreit et al. 2005; disk fragmentation, Goodwin & Whitworth 2007; Stamatellos et al. 2007; or photoevaporation, Whitworth & Zinnecker 2004). Alternatively, brown dwarfs and free-floating planets (with masses below the deuterium-burning mass limit, $\leqslant 13 M_{\rm Jup}$) could form in an isolated mode by direct collapse. This could be possible either introducing turbulence so that the Jeans mass decreases in the first place (Padoan 2002; Hennebelle & Chabrier 2008) or from a filament collapse (e.g., Inutsuka & Miyama 1992) forming low-mass cores that experience high self-erosion in outflows (Machida et al. 2009).

In order to test these models, observational constraints need to be placed on the main features of star formation (disk properties/morphology, accretion, outflows, etc.) toward the lowest possible masses, so that conclusions can be drawn from the behaviors of those properties with the mass of the central object.

Young brown dwarfs were shown to have substantial circumstellar material based on near-infrared (IR; e.g., Oasa et al. 1999; Muench et al. 2001), mid-IR (*ISO* and *Spitzer*; e.g., Natta & Testi 2001; Natta et al. 2002; Apai et al. 2005; Barrado y Navascués et al. 2007; Luhman et al. 2008; Bayo et al. 2012), far-IR (*Herschel*; e.g., Harvey et al. 2012a, 2012b; Alves de Oliveira et al. 2013; Joergens et al. 2013; Liu et al. 2015) and single-dish millimeter continuum photometry (e.g., Klein et al. 2003; Scholz et al. 2006; Mohanty et al. 2013). Only a few years ago, millimeter interferometers became more sensitive, and the disk around 2MJ0444 (M7.25, $\sim 0.05 M_\odot$) was the first of its kind to be spatially resolved at 1.3 mm (CARMA observations by Ricci et al. 2013) with an estimated disk radius of 15–30 au. Even more recently, ALMA allowed several groups to perform small surveys in the substellar domain including intermediate-to-high-mass brown dwarfs (Ricci et al. 2014; Daemgen et al. 2016; Pascucci et al. 2016; Testi et al. 2016; van der Plas et al. 2016). Measurements of low spectral indices of a handful objects showed that dust grains have grown to millimeter sizes even in these very low-mass environments (e.g., Ricci et al. 2013), challenging models of planetesimal formation, which predict that dust growth is more limited by radial drift than in disks around stellar objects (Pinilla et al. 2013). Hints of disk truncation in the substellar domain were presented (Testi et al. 2016), as well as different estimates of the temperature of the dust in substellar disks and an evolution (Andrews et al. 2013; van der Plas et al. 2016), within the first 10 Myr, of the $M_{\rm dust}$–M_* relationship (pointing again toward grain growth, drift, and fragmentation).

Moving down in mass, the lowest-mass isolated objects found to harbor a disk are, to the best of our knowledge, Proplyd 133-353 ($\leqslant 13 M_{\rm Jup}$; Fang et al. 2016), Cha 1109-7734 ($\sim 8 M_{\rm Jup}$; Luhman et al. 2005a), J02265658-5327032 ($\sim 13 M_{\rm Jup}$; Boucher et al. 2016),

and OTS44 ($\sim$12$M_{\rm Jup}$; Joergens et al. 2013), with central object masses well below what has been studied with ALMA until now.

In this Letter, we present the first millimeter detection of one of these four extremely low-mass objects, OTS44. In Section 2, we describe in more detail the target; in Section 3, we describe our observations; in Section 4, we present our disk estimate and the comparison with the literature; and in Section 5, we present our conclusions.

2. OTS44

OTS44 is the object with the latest spectral type in the Chamaeleon I (Cha I) star-forming region (M9.5) with a mass below or close to the planetary border (with estimates from 6 to 17$M_{\rm Jup}$; Luhman et al. 2005b; Bonnefoy et al. 2014). First evidence for a disk around OTS44 came from mid- and far-IR excess emission detected with *Spitzer* and *Herschel* (Luhman et al. 2005b; Harvey et al. 2012a, 2012b). In addition, we observed OTS44 with VLT/SINFONI and detected strong, broad, and variable Pa β emission, which is evidence for active disk accretion in the planetary regime with a relatively high mass-accretion rate ($8 \times 10^{-12}\ M_\odot\ {\rm yr}^{-1}$; Joergens et al. 2013).

We recently determined the properties of the disk of OTS44 (Joergens et al. 2013; Liu et al. 2015) through radiative transfer modeling of its spectral energy distribution from the optical to the far-IR applying the radiative transfer code MC3D (Wolf 2003) and a Bayesian analysis. The disk model that fitted the mid- and far-IR data best was that of a highly flared disk with a dust mass of 0.17$M_\oplus$. However, our far-IR *Herschel* measurements (a detection at 70 μm and an upper limit at 160 μm) are insensitive to millimeter-sized grains, which prevented us from concluding about the presence of large grains (a maximum grain size of 100 μm was assumed in Liu et al. 2015), with this potentially leading to an underestimation of the disk dust mass. In this Letter, we report the first ALMA detection of the disk of a planetary-mass object, providing a more robust estimate of its mass and supporting the idea that the value obtained in Liu et al. (2015) was indeed an underestimation.

3. ALMA Data

ALMA Cycle 3 Band 6 continuum data were obtained as part of the program *2015.1.00243.S*. Four spectral windows (centered at 224, 226, 240, and 242 GHz and each one with $\sim$1.9 GHz bandwidth) were defined to be collapsed in a single "broadband" continuum image.

The data processing was performed with CASA (McMullin et al. 2007), following the standard steps starting from the measurement sets: visual inspection of the performance of antennas and scans, flagging corrupted or useless data (using solutions derived from the water vapor radiometer), correcting in bandpass, flux and phase, further flagging (shadowing, spectral window edges anomalies, etc.), deriving the bandpass solution per spectral window, and creating the cube from the calibrated data (the derived flux uncertainty is $\sim$8%, but, based on the ALMA documentation, we assumed a more conservative 10% value from now on).

In addition to these general steps, we tried to apply self-calibration to improve the extended flux recovery but the signal-to-noise ratio (S/N) of the data was not good enough. Finally, we tried to bin our data in two spectral windows as
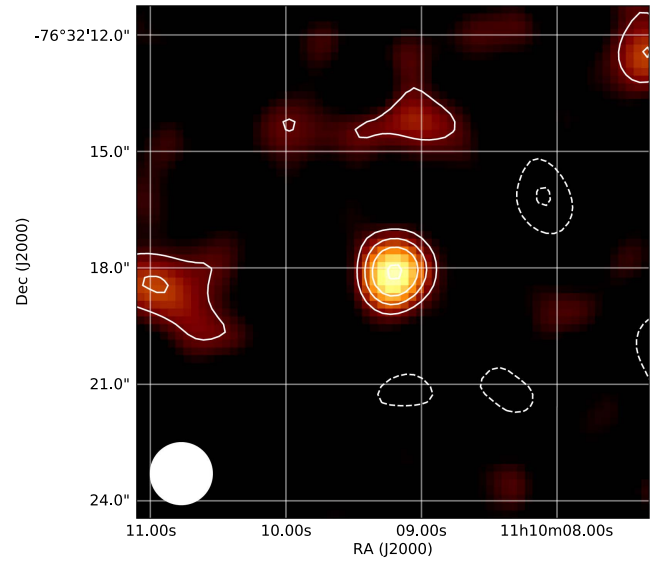

Figure 1. Frequency collapsed ALMA Band 6 data of OTS44. The $1\rlap{.}''6 \times 1\rlap{.}''6$ beam is displayed in the lower left corner. Solid-line white contours highlight regions with 3, 5, 7, and 10 times the rms of the data (9.8 μJy/beam). Dashed-line white contours highlight $-3\times$ rms and $-5\times$ rms regions, and there are no data at the -7 and -10 rms levels.

separated as possible to obtain a spectral index, but once again, the S/N of the data was not good enough for this purpose.

The final CLEAN, primary beam corrected image (natural weighting) has a beam of $1\rlap{.}''6 \times 1\rlap{.}''6$, an rms of 9.8 μJy/beam, a central reference frequency of 233 GHz, and a frequency range covered (not continuously) of 20 GHz. We detected OTS44 as a point-like source with a peak flux value 0.101 ± 0.01 mJy (see Figure 1).

4. Results and Discussion: Dust Disk Mass

The most direct quantity that we can derive from our data is the dust mass of the disk. In this section, we provide such estimates and compare them with the available literature.

4.1. Disk Mass via Analytical Prescription

In order to estimate the disk dust mass from millimeter data, we assume that the emission is optically thin and isothermal at temperature $T_{\rm dust}$, and therefore

$$M_{\rm dust} = \frac{F_\nu \times d^2}{\kappa_\nu \times B_\nu(T_{\rm dust})},$$

where F_ν is the flux density, d is the distance to Cha I (160 pc is assumed; Whittet et al. 1997), κ_ν is the mass absorption coefficient, and B_ν is the Planck function of temperature $T_{\rm dust}$ at the observed frequency.

We have adopted a κ_ν value of 2.3 cm^2 g^{-1} at 230 GHz with a frequency dependence of $\nu^{0.4}$, the same as in Andrews et al. (2013) for Taurus, and more recently by Pascucci et al. (2016) for Cha I. For consistency, we have adapted all $M_{\rm dust}$ values from the literature to be compatible with this assumption.

The remaining strong assumption rests on the choice of $T_{\rm dust}$. A typical value used for $T_{\rm dust}$ is 20 K, but Andrews et al. (2013) showed that this temperature scales significantly with the luminosity of the central object, proposing the relation: $T_{\rm dust} = 25 \times (L_*/L_\odot)^{1/4}$ K. However, this empirical relation yields a temperature of 5.5 K for OTS44 (assuming a
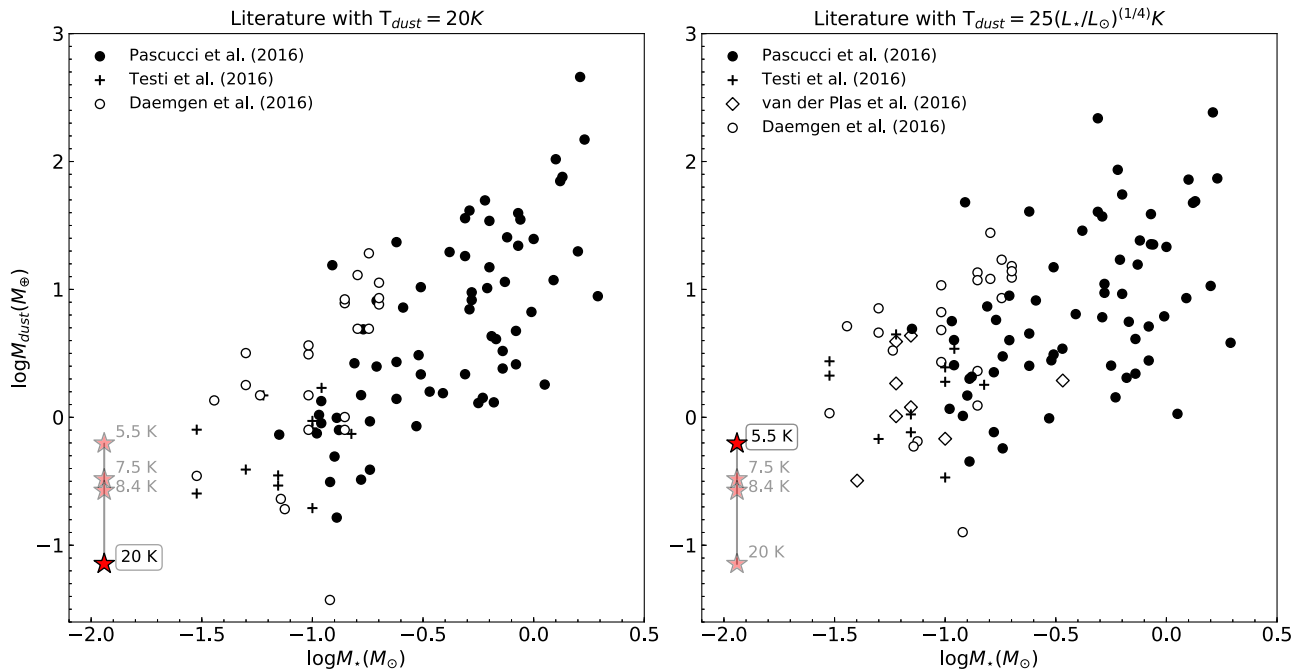
Figure 2. Illustration of the four (five-point red stars) possible determinations of the dust mass of the disk of OTS44 depending on the adopted temperature, in an M_*-M_{disk} diagram, along with comparisons with other substellar objects reported in the literature. In each panel, we outline with a box the corresponding value of T_{dust} assumed for OTS44.

luminosity of 0.0024 $L_\odot$; Joergens et al. 2013), which is unrealistic given the higher temperatures reported merely by heating due to the interstellar radiation field (IRF; Draine 2011). Very recently, van der Plas et al. (2016) revised this dependence as $T_{dust} = 22 \times (L_*/L_\odot)^{0.16}$ K, which translates to a dust temperature of 8.4 K for OTS44 (with the same $L_\odot$ as before).

For completeness we have considered four different temperatures: the "classical" 20 K, the 8.4 K obtained assuming the relationship from van der Plas et al. (2016), that of IRF (7.5 K, Draine 2011), and the 5.5 K derived following the relationship from Andrews et al. (2013). The corresponding estimates for the dust mass of the disk of OTS44 are: 0.07, 0.27, 0.33, and 0.63 $M_\oplus$, respectively.

In Figure 2, we show how our four estimates of the dust mass in the disk around OTS44 compare to literature values for stellar and substellar objects in the literature from Pascucci et al. (2016), van der Plas et al. (2016), Daemgen et al. (2016), and Testi et al. (2016). We note that we are only comparing values derived from interferometric measurements since those derived from single-dish observations tend to be higher pointing toward a contamination of the measurement by the molecular cloud.

The estimates for the different samples shown in Figure 2 are consistent with each other since we recalculated the dust masses using the same absorption coefficient (to rescale the values in Testi et al. 2016). In the case where T_{dust} scales with the bolometric luminosity of the central object, the same caution was taken in the use of consistent opacities, and we adopted the stellar parameters from Manara et al. (2014, 2016) and Manara et al. (2017), for the Pascucci et al. (2016) sample (Cha I objects, as OTS44), where those values are generally in agreement with Luhman (2004) or more recently Bayo et al. (2017).

The conclusion from these comparisons is that a "very high" T_{dust} value of 20 K translates in an extremely low-mass disk that would fall in the lower envelope of the M_*-M_{disk} relationship drawn by the literature data. However, 20 K is probably an unrealistic value for the dust temperature unless disks around these very low-mass central objects are much smaller and flared than those around low-mass stars, a trend challenged, for example, by Liu et al. (2015), but worthy of further scrutiny. On the other hand, values between 5.5 and 8.4 K yield disk masses compatible with the dispersion observed in the literature data (although 5.5 K is probably also unrealistic due to the fact that including an IRF already brings this value to 7.5 K), pushing the M_*-M_{disk} correlation into, or at the border of, the planetary-mass domain.

5. Conclusions

We have presented the first millimeter detection of the dusty disk around an isolated planetary-mass object. Taking into account the strong assumptions to derive its dust mass, and following different approaches to do so, the values we obtain are consistent with the log–log linear relation between M_* and M_{dust}, holding even at the planetary-mass domain.

However, these mass estimates are severely limited by assumptions on poorly constrained parameters such as the dust properties in disks around these extremely low-mass objects. In addition, crucial aspects such as grain growth cannot be probed with one-band millimeter observations. To tackle these questions, the ideal complementary data would include $\sim 200\,\mu$m (unfortunately, most likely beyond the limits of ALMA Band 10, ~ 869 GHz, capabilities) observations and extremely sensitive ALMA Band 3 observations.

References

Alves de Oliveira, C., Ábrahám, P., Marton, G., et al. 2013, A&A, 559, A126
Andrews, S. M., Rosenfeld, K. A., Kraus, A. L., & Wilner, D. J. 2013, ApJ, 771, 129
Apai, D., Pascucci, I., Bouwman, J., et al. 2005, Sci, 310, 834
Astropy Collaboration, Robitaille, T. P., Tollerud, E. J., et al. 2013, A&A, 558, A33
Barrado y Navascués, D., Stauffer, J. R., Morales-Calderón, M., et al. 2007, ApJ, 664, 481
Bayo, A., Barrado, D., Allard, F., et al. 2017, MNRAS, 465, 760
Bayo, A., Barrado, D., Huélamo, N., et al. 2012, A&A, 547, A80
Bonnefoy, M., Chauvin, G., Lagrange, A.-M., et al. 2014, A&A, 562, A127
Boucher, A., Lafrenière, D., Gagné, J., et al. 2016, ApJ, 832, 50
Daemgen, S., Natta, A., Scholz, A., et al. 2016, A&A, 594, A83
Draine, B. T. 2011, ApJ, 732, 100
Fang, M., Kim, J. S., Pascucci, I., Apai, D., & Manara, C. F. 2016, ApJL, 833, L16
Goodwin, S. P., & Whitworth, A. 2007, A&A, 466, 943
Harvey, P. M., Henning, T., Liu, Y., et al. 2012b, ApJ, 755, 67
Harvey, P. M., Henning, T., Ménard, F., et al. 2012a, ApJL, 744, L1
Hennebelle, P., & Chabrier, G. 2008, ApJ, 684, 395
Inutsuka, S.-I., & Miyama, S. M. 1992, ApJ, 388, 392
Joergens, V., Bonnefoy, M., Liu, Y., et al. 2013, A&A, 558, L7
Klein, R., Apai, D., Pascucci, I., Henning, T., & Waters, L. B. F. M. 2003, ApJL, 593, L57
Liu, Y., Joergens, V., Bayo, A., Nielbock, M., & Wang, H. 2015, A&A, 582, A22
Luhman, K. L. 2004, ApJ, 602, 816
Luhman, K. L., Adame, L., D'Alessio, P., et al. 2005a, ApJL, 635, L93
Luhman, K. L., D'Alessio, P., Calvet, N., et al. 2005b, ApJL, 620, L51
Luhman, K. L., Hernández, J., Downes, J. J., Hartmann, L., & Briceño, C. 2008, ApJ, 688, 362
Machida, M. N., Inutsuka, S.-i., & Matsumoto, T. 2009, ApJL, 699, L157
Manara, C. F., Fedele, D., Herczeg, G. J., & Teixeira, P. S. 2016, A&A, 585, A136
Manara, C. F., Testi, L., Herczeg, G. J., et al. 2017, A&A, in press (arXiv:1704.02842)
Manara, C. F., Testi, L., Natta, A., et al. 2014, A&A, 568, A18
McMullin, J. P., Waters, B., Schiebel, D., Young, W., & Golap, K. 2007, in ASP Conf. Ser. 376, Astronomical Data Analysis Software and Systems XVI, ed. R. A. Shaw, F. Hill, & D. J. Bell (San Francisco, CA: ASP), 127
Mohanty, S., Greaves, J., Mortlock, D., et al. 2013, ApJ, 773, 168
Muench, A. A., Alves, J., Lada, C. J., & Lada, E. A. 2001, ApJL, 558, L51
Natta, A., & Testi, L. 2001, A&A, 376, L22
Natta, A., Testi, L., Comerón, F., et al. 2002, A&A, 393, 597
Oasa, Y., Tamura, M., & Sugitani, K. 1999, ApJ, 526, 336
Ochsenbein, F., Bauer, P., & Marcout, J. 2000, A&AS, 143, 23
Padoan, P., & Nordlund, Å. 2002, ApJ, 576, 870
Pascucci, I., Testi, L., Herczeg, G. J., et al. 2016, ApJ, 831, 125
Pinilla, P., Birnstiel, T., Benisty, M., et al. 2013, A&A, 554, A95
Reipurth, B., & Clarke, C. 2001, AJ, 122, 432
Ricci, L., Isella, A., Carpenter, J. M., & Testi, L. 2013, ApJL, 764, L27
Ricci, L., Testi, L., Natta, A., et al. 2014, ApJ, 791, 20
Scholz, A., Jayawardhana, R., & Wood, K. 2006, ApJ, 645, 1498
Stamatellos, D., Hubber, D. A., & Whitworth, A. P. 2007, MNRAS, 382, L30
Testi, L., Natta, A., Scholz, A., et al. 2016, A&A, 593, A111
Umbreit, S., Burkert, A., Henning, T., Mikkola, S., & Spurzem, R. 2005, ApJ, 623, 940
van der Plas, G., Ménard, F., Ward-Duong, K., et al. 2016, ApJ, 819, 102
Whittet, D. C. B., Prusti, T., Franco, G. A. P., et al. 1997, A&A, 327, 1194
Whitworth, A. P., & Zinnecker, H. 2004, A&A, 427, 299
Wolf, S. 2003, CoPhC, 150, 99